Large-N_c and renormalization group constraints on parity-violating low-energy coefficients for three-derivative operators in pionless effective field theory

Son T. Nguyen [1,*] Matthias R. Schindler [2,†] Roxanne P. Springer [1,‡] and Jared Vanasse [3,§]

[1]*Department of Physics, Duke University, Durham, North Carolina 27708, USA*

[2]*Department of Physics and Astronomy, University of South Carolina, Columbia, South Carolina 29208, USA*

[3]*Fitchburg State University, Fitchburg, Massachusetts 01420, USA*

(Received 9 December 2020; revised 20 March 2021; accepted 12 April 2021; published 27 May 2021)

We extend, from operators with one derivative to operators with three derivatives, the analysis of two-body hadronic parity violation in a combined pionless effective field theory (EFT$_{\not\pi}$) and large-N_c expansion, where N_c is the number of colors in quantum chromodynamics (QCD). In elastic scattering, these operators contribute to S-P and P-D wave transitions, with five operators and their accompanying low energy coefficients (LECs) characterizing the S-P transitions and six operators and LECs those in P-D transitions. We show that the large-N_c analysis separates them into leading order in N_c, next-to-leading order in N_c, etc. Relationships among EFT$_{\not\pi}$ LECs emerge in the large-N_c expansion. We also discuss the renormalization group (RG) scale dependence of these LECs by considering two distinct limits: one in which large-N_c relationships among LECs hold but RG-related approximate expansions do not, and vice versa. Our analysis can complement lattice QCD calculations and help prioritize future parity-violating experiments.

DOI: 10.1103/PhysRevC.103.054004

I. INTRODUCTION

Understanding weak interactions in few-nucleon systems may provide a window into how nonperturbative quantum chromodynamics (QCD) governs nuclear structure and behavior. Since parity is conserved in electromagnetic and strong interactions but not in weak interactions, parity-violating (PV) processes involving few nucleons can be used to isolate the effects of the weak interactions, which are suppressed by about seven orders of magnitude relative to the strong interactions (see, e.g., [1–5] and their references for theoretical reviews and experimental status). The nonperturbative nature of QCD at low energies makes direct calculations of hadronic PV observables challenging. While lattice QCD efforts in this direction continue, they are still in their infancy [6,7]. Effective field theories (EFTs) provide a model-independent approach for understanding interactions among nucleons.

EFTs exploit any hierarchy of scales existing in a system. They retain dynamics that are relevant at the desired energy scale as well as underlying symmetries, while all high-energy/short-distance dynamics are encoded into low-energy coefficients (LECs), which are not determined by these symmetries. The LECs may be calculated from the underlying theory or fit to experimental data. At any given order in the EFT expansion, only a finite number of LECs are relevant. Once these have been fixed by comparison with data, their values can be used to predict additional observables.

At momenta significantly below the pion mass ($m_\pi \approx 140$ MeV), an EFT describing few-nucleon physics may be constructed in which the only dynamical degrees of freedom are nonrelativistic nucleons and possibly photons, neutrinos, etc. In this pionless EFT (EFT$_{\not\pi}$) [8–15], the operators are organized in powers of $p/\Lambda_{\not\pi}$, where p is a typical external momentum or momentum transfer in the system, and $\Lambda_{\not\pi} \sim m_\pi$ is the breakdown scale of EFT$_{\not\pi}$. When restricted to two-nucleon processes, EFT$_{\not\pi}$ is written in terms of four-nucleon contact interactions, with terms involving an adequate number of derivatives to reach the desired level of precision. EFT$_{\not\pi}$ is well established for the low-energy regime of $E \lesssim 10$ MeV in the laboratory frame (or momentum transfers of $p \ll \Lambda_{\not\pi}$). (For reviews, see Refs. [16–21].)

Another useful tool for understanding QCD is the large-N_c limit, where the number of colors, N_c, is taken to be large (the physical value is $N_c = 3$) [22,23]. Combining the large-N_c expansion with the EFT$_{\not\pi}$ expansion puts constraints on the LECs of EFT$_{\not\pi}$. The approach of combining EFT$_{\not\pi}$ with large N_c has been applied to parity-conserving (PC) nucleon-nucleon (NN) interactions [24–26], the leading (largest) PV NN interactions [27], time-reversal violating NN interactions [28], and interactions with external currents [29]. In this paper, we use the dual EFT$_{\not\pi}$ and large-N_c expansion to study the impact of three-derivative operators on PV NN interactions. The leading PV NN terms appear with one derivative and

*stn7@phy.duke.edu
†mschindl@mailbox.sc.edu
‡rps@phy.duke.edu
§jvanass3@fitchburgstate.edu

describe S-P wave transitions. For elastic scattering, five independent three-derivative operators provide corrections to these S-P wave transitions, and an additional six independent three-derivative operators contain the leading contributions to P-D wave transitions.

At present, there exist two measurements of PV two-nucleon observables performed at the low energies where EFT$_{\not\pi}$ is valid. The longitudinal asymmetry in $\vec{p}p$ scattering was found in Refs. [30,31]. More recently, the NPDGamma Collaboration published the PV gamma-ray asymmetry arising from polarized neutron capture on the proton [32]. Contributions from P-D transitions to PV asymmetries become competitive with those from S-P transitions at high enough energies. A measurement of PV pp scattering was performed at 221 MeV [33,34] since the contributions from S-P transitions were expected to be at a minimum at this energy. However, EFT$_{\not\pi}$ is not valid at such high energies. One approach to extract P-D transitions at low energies is to look at the angular correlations within PV asymmetries. For example, taking the difference divided by the sum of the differential scattering cross sections for a forwards and backwards longitudinally polarized neutron beam on an unpolarized proton target would give a PV asymmetry with angular dependence. From this angular information, the P-D LECs could in principle be extracted. However, this would require higher statistics than is needed to extract leading S-P LECs and would be a difficult experiment. Certain asymmetries at low energies may be sensitive to P-D transitions due either to a fortuitous suppression of S-P transitions and/or enhancement of P-D transitions. It is not clear, short of careful study, what, if any, asymmetries may do this and such asymmetries may be as difficult to measure as the angular dependence in other asymmetries.

The dual EFT$_{\not\pi}$ and large-N_c expansion has been successfully applied in the PC sector [24–26], in which sufficient data are available to test its predictions. While data are much more sparse in the PV sector, the existing results for the PV EFTs are not incompatible with the large-N_c picture. An isovector LEC can be extracted from the NPDGamma result [32] and is relatively small, as expected from a term that is next-to-leading order (NLO) in the large-N_c expansion [27]. In addition, Ref. [27] showed that an experimental bound on the induced circular polarization in unpolarized neutron capture ($np \to d\vec{\gamma}$) [35,36] indicates that an isoscalar and an isotensor LEC are of the same size, as suggested by that large-N_c analysis.

If the dual expansion can be used to indicate which PV terms are most important, it may help prioritize future PV experiments. For the interactions considered here, the dual expansion yields an estimate of which of the 11 three-derivative operators will be dominant; the large-N_c expansion suggests that only two of these EFT$_{\not\pi}$ LECs are both dominant and independent. This allows us to obtain corrections to the leading S-P LEC relationships found in Ref. [27] and provides constraints for P-D LECs as well. However, at the moment, there is no experimental evidence available to verify these predictions. Nonetheless, this work provides a model-independent analysis of low-energy P-D transitions. This is an important benchmark since any theory that is valid at higher energies will need to match these results in the low-energy limit.

Since this is the first detailed study of three-derivative operators in EFT$_{\not\pi}$, we investigate the renormalization group (RG) behavior of the corresponding LECs. Our analysis shows that PV scattering does not require a new LEC until two orders past leading. Further, we see that the PV LEC RG equations have a general form, paralleling that found in the PC sector [11,12,14]. These equations hold independent of the value of the subtraction point μ.

A subtlety of the large-N_c analysis is that it applies not to observables but to LECs, which are typically μ dependent. Previous results, from the PC sector [24,26], suggest that large-N_c constraints on LECs only hold at values of μ around or above the pion mass. Therefore, in addition to studying general RG behavior, we also consider how the LECs behave when $\mu > m_\pi$ versus an incompatible limiting case, $\mu \ll m_\pi$. In the latter limit, approximations in the RG equations yield relationships among LECs in different channels. We expect that one or the other of these regions may be useful to help reduce the number of independent LECs needed to understand a given process.

Potential future experiments, e.g., at the high-intensity cold neutron beam line at the Spallation Neutron Source at the Oak Ridge National Laboratory and the High-Intensity Gamma-ray Source at the Triangle Universities Nuclear Laboratory [37,38], are expected to provide additional information on the PV LECs. At the same time, there are attempts to calculate PV LECs using lattice QCD [6,7,39]. The isotensor terms in particular present an opportunity for lattice QCD because the calculation does not involve disconnected (quark-loop) diagrams. As shown in Refs. [27,40], isotensor contributions are dominant in large-N_c counting; they are particularly attractive for lattice QCD and future experiments.

An outline of this paper is as follows: we begin with a brief review of the large-N_c counting rules in Sec. II. In Sec. III, we introduce the PV Lagrangian expressed in two different bases: one in which the large-N_c scaling is most transparent, the other describing the interactions in terms of partial-wave transitions. We will refer to these as the large-N_c and partial-wave bases, respectively. The large-N_c scaling of the partial-wave LECs is then provided. We discuss the RG behaviors of LECs and apply them to available experimental data in Sec. IV. Conclusions and an Appendix showing an example Fierz procedure follow.

II. LARGE-N_c COUNTING

Using the large-N_c limit of QCD to understand hadron properties was first suggested by t'Hooft [22] and further developed by Witten [23]. Assuming a sensible $N_c \to \infty$ limit exists, $1/N_c$ may serve as a useful expansion parameter for large, but finite N_c. Many calculations have demonstrated the capability of this method to make definite predictions of meson and baryon dynamics (see, e.g., Refs. [41–43] for reviews).

In the large-N_c approach, baryons consist of N_c quarks. Quark confinement requires that the baryon wave function be an SU(N_c) color singlet. Since the total wave function of the baryon must be completely antisymmetric, the baryon's ground-state wave function is totally symmetric in

spin and flavor components. This motivates the introduction of so-called bosonic quarks from which the color degrees of freedom are removed. Neutrons and protons consist of valence up (u) and down (d) quarks, which can each be in two possible spin states ($\uparrow, \downarrow$). References [44–50] showed that in the $N_c \to \infty$ limit, there is an SU(4) spin-flavor symmetry with $u\uparrow, u\downarrow, d\uparrow$, and $d\downarrow$ in the fundamental representation, where u and d are the bosonic quarks. In the large-N_c limit, NN interactions take the form of a Hartree Hamiltonian [23–25,47]:

$$\hat{H} = N_c \sum_{n=0}^{N_c} \sum_{s+t\leqslant n} v_{stn}(\mathbf{p},\mathbf{p}')\left(\frac{\hat{S}}{N_c}\right)^s \left(\frac{\hat{I}}{N_c}\right)^t \left(\frac{\hat{G}}{N_c}\right)^{n-s-t}, \quad (1)$$

where v_{stn} is a function of momenta and scales, at most, as $O(N_c^0)$ in the large-N_c counting. The operators in Eq. (1) and the identity are

$$\hat{S}_i = \hat{q}^\dagger \frac{\sigma_i \otimes \mathbb{1}}{2}\hat{q}, \quad \hat{I}_a = \hat{q}^\dagger \frac{\mathbb{1}\otimes\tau_a}{2}\hat{q},$$
$$\hat{G}_{ia} = \hat{q}^\dagger \frac{\sigma_i \otimes \tau_a}{4}\hat{q}, \quad \hat{\mathbb{1}} = \hat{q}^\dagger(\mathbb{1}\otimes\mathbb{1})\hat{q}, \quad (2)$$

where $\hat{q} = (u, d)$ are bosonic quarks, and σ_i, τ_a are SU(2) Pauli matrices ($i, a = 1, 2, 3$) acting on spin and isospin spaces, respectively. When evaluated between nucleon states, the large-N_c counting rules for matrix elements of the spin-isospin operators and the identity are given by [24,25,47]

$$\langle N'|\hat{S}_i/N_c|N\rangle \sim \langle N'|\hat{I}_a/N_c|N\rangle \lesssim N_c^{-1},$$
$$\langle N'|\hat{G}_{ia}/N_c|N\rangle \sim \langle N|\hat{\mathbb{1}}/N_c|N\rangle \lesssim N_c^0, \quad (3)$$

where $N = (p, n)^T$ is the nucleon field.

The potential between two nucleons can be viewed as a matrix element of the above Hartree Hamiltonian [25]. In the center-of-mass (c.o.m.) frame,

$$V = \langle \mathbf{p}'; -\mathbf{p}'|\hat{H}|\mathbf{p}; -\mathbf{p}\rangle. \quad (4)$$

Two independent momentum variables can be defined [25],

$$\mathbf{p}_+ = \mathbf{p} + \mathbf{p}', \quad \mathbf{p}_- = \mathbf{p} - \mathbf{p}'. \quad (5)$$

How momenta scale with N_c is a subject of much debate [23,51]. As discussed in Ref. [51], one argument can be made using the meson-exchange potential derived from the Hartree Hamiltonian. Considering the t channel, $\mathbf{p}_+$ only results from relativistic corrections and therefore contributes to the N_c counting as $1/M \sim 1/N_c$ since the nucleon mass M scales as N_c [23]. The large-N_c counting of momenta in this channel then becomes

$$\mathbf{p}_- \sim N_c^0, \quad \mathbf{p}_+ \sim N_c^{-1}. \quad (6)$$

The analysis in the u channel is complementary, so we will restrict the discussion to the t channel. Equations (3) and (6) are sufficient to systematically determine which spin-isospin structures occur at each large-N_c order. We will use this to describe two-nucleon PV scattering, retaining rotational and time-reversal invariance. A concise overview of the transformation properties of various spin-isospin operators can be found in Tables I and II of Ref. [52]. These constraints restrict the possible terms in the PV potential. In the next section, following the procedure used in Ref. [27], we present the EFT$_{\not\pi}$ PV Lagrangian with three derivatives and obtain the large-N_c scaling of the relevant LECs.

III. EFT$_{\not\pi}$ PARITY-VIOLATING LAGRANGIAN WITH THREE DERIVATIVES

At three derivatives, the effective two-nucleon interactions are characterized by dimension-nine operators. The choice of basis used to express these operators is arbitrary. As long as the underlying symmetries are obeyed, different choices of bases must yield the same physics. However, as is often the case, some basis choices are more illuminating than others.

In this paper, we will consider the PV EFT$_{\not\pi}$ Lagrangian in two bases: the large-N_c basis, expressed in the form $(N^\dagger \mathcal{O}_1 N)(N^\dagger \mathcal{O}_2 N)$, and the partial-wave basis, expressed in the form $(N^T \mathcal{O}_3 N)^\dagger (N^T \mathcal{O}_4 N)$, where the $\mathcal{O}_i$ are spin-isospin and momentum operators. While the physics might be more transparent in the partial-wave basis, the large-N_c scaling can be most easily determined in the large-N_c basis. Fierz identities can be used to transform between these two bases, but this must be done with care in order to maintain the correct large-N_c ordering of the operators.

A. Large-N_c basis Lagrangian

The terms in the PV three-derivative Lagrangian that appear at leading order (LO) in the large-N_c expansion are given in the large-N_c basis by

$$\mathcal{L}_{\rm LO} = C^{[3]}_{G.G}\epsilon_{ijk}\nabla_i(N^\dagger\sigma_j\tau_a N)\nabla^2(N^\dagger\sigma_k\tau_a N) + C'^{[3]}_{G.G}\epsilon_{ijk}\mathcal{I}_{ab}\nabla_i(N^\dagger\sigma_j\tau_a N)\nabla^2(N^\dagger\sigma_k\tau_b N), \quad (7)$$

corresponding to a potential

$$V_{\rm LO} = -iC^{[3]}_{G.G}\,\mathbf{p}_-^2\,\mathbf{p}_-\cdot(\vec{\sigma}_1\times\vec{\sigma}_2)(\vec{\tau}_1\cdot\vec{\tau}_2) - iC'^{[3]}_{G.G}\,\mathbf{p}_-^2\,\mathbf{p}_-\cdot(\vec{\sigma}_1\times\vec{\sigma}_2)(\tau_1^a\mathcal{I}_{ab}\tau_2^b). \quad (8)$$

Here, $\mathcal{I}_{ab} = \mathrm{diag}(1, 1, -2)$, and $C^{[3]}_{G.G}$, $C'^{[3]}_{G.G}$ are two LECs with subscripts chosen to reflect the operator structures they accompany. These two terms describe isospin transitions $\Delta I = 0$ and $\Delta I = 2$, respectively. The rules of Eqs. (3) and (6) yield the N_c scaling of the two couplings,

$$C^{[3]}_{G.G} \sim N_c, \quad C'^{[3]}_{G.G} \sim N_c, \quad (9)$$

where a factor of $\sin^2\theta_W \approx 0.23$ [53] in the isotensor coupling could be included because of matching at the weak scale [27,40]. However, it is not clear that this suppression survives the strong running to the low-energy scales that we consider. At NLO, scaling as N_c^0 in large N_c, there are four $\Delta I = 1$ operators,

$$\mathcal{L}_{\rm NLO} = \frac{1}{2}\widetilde{C}^{[3]}_{G.\sigma}\epsilon_{ijk}[\nabla_i(N^\dagger\sigma_j\tau_3 N)\nabla^2(N^\dagger\sigma_k N) + \nabla_i(N^\dagger\sigma_j N)\nabla^2(N^\dagger\sigma_k\tau_3 N)] + \frac{1}{2}\widetilde{C}^{[3]}_{G.\tau}\epsilon_{ab3}\big[\nabla_i(N^\dagger\sigma_i\tau_a N)\nabla^2(N^\dagger\tau_b N) + \nabla_i(N^\dagger\tau_a N)\nabla^2(N^\dagger\sigma_i\tau_b N)\big]$$

$$+\widetilde{C}^{[3]}_{G.G}\epsilon_{ijk}\epsilon_{ab3}[(N^\dagger\sigma_i\tau_a i\overleftrightarrow{\nabla}_j N)\nabla_k\nabla_l(N^\dagger\sigma_l\tau_b N)+(N^\dagger\sigma_l\tau_a i\overleftrightarrow{\nabla}_j N)\nabla_k\nabla_l(N^\dagger\sigma_i\tau_b N)]$$
$$+\widetilde{C}^{[3]}_{G.1}[(N^\dagger\sigma_i\tau_3 i\overleftrightarrow{\nabla}_i N)\nabla^2(N^\dagger N)-(N^\dagger i\overleftrightarrow{\nabla}_i N)\nabla^2(N^\dagger\sigma_i\tau_3 N)]. \tag{10}$$

The tilde symbol indicates NLO in large N_c. The Galilean-invariant derivative $\overleftrightarrow{\nabla}$ is defined by $N^\dagger\mathcal{O}\overleftrightarrow{\nabla}_i N\equiv N^\dagger\mathcal{O}(\nabla_i N)-(\nabla_i N^\dagger)\mathcal{O}N$, where $\mathcal{O}$ is a spin-isospin operator. Again, the $\Delta I=1$ terms may be accompanied by a factor of $\sin^2\theta_W$ [27,40] from matching at the weak scale. The corresponding NLO potential is

$$V_{\rm NLO}=-\frac{i}{2}\widetilde{C}^{[3]}_{G.\sigma}\mathbf{p}_-^2\,\mathbf{p}_-\cdot(\vec\sigma_1\times\vec\sigma_2)(\tau_1+\tau_2)^3-\frac{i}{2}\widetilde{C}^{[3]}_{G.\tau}\mathbf{p}_-^2\,\mathbf{p}_-\cdot(\vec\sigma_1+\vec\sigma_2)(\vec\tau_1\times\vec\tau_2)^3$$
$$+\widetilde{C}^{[3]}_{G.G}\big[(\mathbf{p}_+\times\mathbf{p}_-)\cdot\vec\sigma_1\mathbf{p}_-\cdot\vec\sigma_2+\mathbf{p}_-\cdot\vec\sigma_1(\mathbf{p}_+\times\mathbf{p}_-)\cdot\vec\sigma_2\big](\vec\tau_1\times\vec\tau_2)^3+\widetilde{C}^{[3]}_{G.1}\mathbf{p}_-^2\,\mathbf{p}_+\cdot(\vec\sigma_1\tau_1^3-\vec\sigma_2\tau_2^3). \tag{11}$$

There are additional operators at higher orders in the large-N_c expansion; however, in the following, we restrict the discussion to the terms of Eqs. (7) and (10), which are expected to be dominant in the large-N_c expansion. The terms in Eqs. (8) and (11), as well as the terms at next-to-next-to-leading order (NNLO) in the large-N_c expansion, can be obtained from the expressions in Ref. [40] by expanding their functions $U_P^i(\mathbf{p}_-)$ and $U_D^1(\mathbf{p}_-)$ in $\mathbf{p}_-$ and retaining all terms with three powers of momentum.

B. Partial-wave basis Lagrangian

The PV *NN* interactions can also be expressed in terms of the mixing of odd and even partial waves characterized by the spectroscopic notation $^{2S+1}L_J$. During the scattering process, the total angular momentum (orbital plus spin angular momentum) quantum number $J=0,1,2$ of the two-nucleon system must be conserved. The three-derivative PV *NN* interactions can be written in the partial-wave basis as

$$\mathcal{L}^{[3]}_{SP}=\frac{1}{8}\Big[C^{(^3S_1^{[2]}-{}^1P_1^{[1]})}(N^T P_i\overleftrightarrow{\nabla}^2 N)^\dagger(N^T P_0 i\overleftrightarrow{\nabla}_i N)+C^{(^1S_0^{[2]}-{}^3P_0^{[1]})}_{\Delta I=0}(N^T P_a\overleftrightarrow{\nabla}^2 N)^\dagger(N^T P_{i,a} i\overleftrightarrow{\nabla}_i N)$$
$$+C^{(^1S_0^{[2]}-{}^3P_0^{[1]})}_{\Delta I=1}\epsilon_{ab3}(N^T P_a\overleftrightarrow{\nabla}^2 N)^\dagger(N^T P_{i,b}\overleftrightarrow{\nabla}_i N)+C^{(^1S_0^{[2]}-{}^3P_0^{[1]})}_{\Delta I=2}\mathcal{I}_{ab}(N^T P_a\overleftrightarrow{\nabla}^2 N)^\dagger(N^T P_{i,b} i\overleftrightarrow{\nabla}_i N)$$
$$+C^{(^3S_1^{[2]}-{}^3P_1^{[1]})}\epsilon_{ijk}(N^T P_i\overleftrightarrow{\nabla}^2 N)^\dagger(N^T P_{k,3}\overleftrightarrow{\nabla}_j N)+C^{(^3S_1^{[0]}-{}^1P_1^{[3]})}(N^T P_i N)^\dagger(N^T P_0 i\overleftrightarrow{\nabla}_i\overleftrightarrow{\nabla}^2 N)$$
$$+C^{(^1S_0^{[0]}-{}^3P_0^{[3]})}_{\Delta I=0}(N^T P_a N)^\dagger(N^T P_{i,a} i\overleftrightarrow{\nabla}_i\overleftrightarrow{\nabla}^2 N)+C^{(^1S_0^{[0]}-{}^3P_0^{[3]})}_{\Delta I=1}\epsilon_{ab3}(N^T P_a N)^\dagger(N^T P_{i,b}\overleftrightarrow{\nabla}_i\overleftrightarrow{\nabla}^2 N)$$
$$+C^{(^1S_0^{[0]}-{}^3P_0^{[3]})}_{\Delta I=2}\mathcal{I}_{ab}(N^T P_a N)^\dagger(N^T P_{i,b} i\overleftrightarrow{\nabla}_i\overleftrightarrow{\nabla}^2 N)+C^{(^3S_1^{[0]}-{}^3P_1^{[3]})}\epsilon_{ijk}(N^T P_i N)^\dagger(N^T P_{k,3}\overleftrightarrow{\nabla}_j\overleftrightarrow{\nabla}^2 N)\Big]+\text{H.c.}, \tag{12}$$

$$\mathcal{L}^{[3]}_{PD}=\frac{1}{8}\Big[C_3^{(^1P_1-{}^3D_1)}(N^T P_i\overleftrightarrow{\nabla}_x\overleftrightarrow{\nabla}_y N)^\dagger(N^T P_0 i\overleftrightarrow{\nabla}_j N)\Big(\delta_{ix}\delta_{jy}-\frac{1}{3}\delta_{ij}\delta_{xy}\Big)$$
$$+C_3^{(^3P_1-{}^3D_1)}\epsilon_{ijk}(N^T P_l\overleftrightarrow{\nabla}_x\overleftrightarrow{\nabla}_y N)^\dagger(N^T P_{k,3}\overleftrightarrow{\nabla}_j N)\Big(\delta_{lx}\delta_{iy}-\frac{1}{3}\delta_{il}\delta_{xy}\Big)$$
$$+C^{(^3P_2-{}^1D_2)}_{3,\Delta I=0}(N^T P_a\overleftrightarrow{\nabla}_x\overleftrightarrow{\nabla}_y N)^\dagger(N^T P_{i,a} i\overleftrightarrow{\nabla}_j N)\Big(\delta_{ix}\delta_{jy}-\frac{1}{3}\delta_{ij}\delta_{xy}\Big)$$
$$+C^{(^3P_2-{}^1D_2)}_{3,\Delta I=1}\epsilon_{ab3}(N^T P_a\overleftrightarrow{\nabla}_x\overleftrightarrow{\nabla}_y N)^\dagger(N^T P_{i,b}\overleftrightarrow{\nabla}_j N)\Big(\delta_{ix}\delta_{jy}-\frac{1}{3}\delta_{ij}\delta_{xy}\Big)$$
$$+C^{(^3P_2-{}^1D_2)}_{3,\Delta I=2}\mathcal{I}_{ab}(N^T P_a\overleftrightarrow{\nabla}_x\overleftrightarrow{\nabla}_y N)^\dagger(N^T P_{i,b} i\overleftrightarrow{\nabla}_j N)\Big(\delta_{ix}\delta_{jy}-\frac{1}{3}\delta_{ij}\delta_{xy}\Big)$$
$$+C_3^{(^3P_2-{}^3D_2)}\epsilon_{ijk}(N^T P_j\overleftrightarrow{\nabla}_k\overleftrightarrow{\nabla}_l N)^\dagger(N^T P_{m,3}\overleftrightarrow{\nabla}_n N)(\delta_{im}\delta_{ln}+\delta_{in}\delta_{lm})\Big]+\text{H.c.} \tag{13}$$

On the left-hand side, the subscript denotes the partial waves involved in the transition, and the superscript indicates the number of derivatives in the operators. On the right-hand side, the LEC labels are chosen to echo the incoming/outgoing partial waves, and the superscript $[k]$ on a particular channel indicates the number of derivatives acting on that partial-wave channel. ΔI denotes the isospin structure of the operator. The operators between nucleon fields are projectors onto the required combination of spin and isospin. The partial-wave projectors and momentum structures are provided in Ref. [54],

$$P_i=\frac{1}{\sqrt{8}}\sigma_2\sigma_i\tau_2,\quad P_a=\frac{1}{\sqrt{8}}\sigma_2\tau_2\tau_a,$$
$$P_{i,a}=\frac{1}{\sqrt{8}}\sigma_2\sigma_i\tau_2\tau_a,\quad P_0=\frac{1}{\sqrt{8}}\sigma_2\tau_2. \tag{14}$$

In general, the magnitudes of the relative momenta of the incoming and outgoing nucleons are not equal, i.e., $|\mathbf{p}|\neq|\mathbf{p}'|$. But for elastic scattering, the two operators with different

TABLE I. Large-N_c scaling of and mapping between large-N_c and partial-wave bases.

LEC		LO in N_c, $O(N_c)$		NLO in N_c, $O(N_c^0)$
$C_3^{(^3S_1-{}^1P_1)}$	=	$32C_{G.G}^{[3]}$	+	0
$C_{3,\Delta I=0}^{(^1S_0-{}^3P_0)}$	=	$\frac{32}{3}C_{G.G}^{[3]}$	+	0
$C_{3,\Delta I=1}^{(^1S_0-{}^3P_0)}$	=	0	+	$\frac{16}{3}(2\widetilde{C}_{G.\sigma}^{[3]}+\widetilde{C}_{G.1}^{[3]})$
$C_{3,\Delta I=2}^{(^1S_0-{}^3P_0)}$	=	$-\frac{64}{3}C'^{[3]}_{G.G}$	+	0
$C_3^{(^3S_1-{}^3P_1)}$	=	0	+	$-\frac{16}{3}(2\widetilde{C}_{G.\tau}^{[3]}+\widetilde{C}_{G.1}^{[3]})$
$C_3^{(^1P_1-{}^3D_1)}$	=	$24C_{G.G}^{[3]}$	+	0
$C_3^{(^3P_1-{}^3D_1)}$	=	0	+	$4(\widetilde{C}_{G.\tau}^{[3]}-\widetilde{C}_{G.1}^{[3]}-6\widetilde{C}_{G.G}^{[3]})$
$C_{3,\Delta I=0}^{(^3P_2-{}^1D_2)}$	=	$8C_{G.G}^{[3]}$	+	0
$C_{3,\Delta I=1}^{(^3P_2-{}^1D_2)}$	=	0	+	$8(\widetilde{C}_{G.\sigma}^{[3]}-\widetilde{C}_{G.1}^{[3]})$
$C_{3,\Delta I=2}^{(^3P_2-{}^1D_2)}$	=	$-16C'^{[3]}_{G.G}$	+	0
$C_3^{(^3P_2-{}^3D_2)}$	=	0	+	$4(-\widetilde{C}_{G.\tau}^{[3]}+\widetilde{C}_{G.1}^{[3]}-2\widetilde{C}_{G.G}^{[3]})$

placements of $\overleftrightarrow{\nabla}^2$ in each S-P transition cannot be distinguished; the LECs occur in the linear combination $C^{(S^{[2]}-P^{[1]})}+C^{(S^{[0]}-P^{[3]})}$. Going forward, we will use the new set of LECs,

$$C_3^{(SP)}\equiv C^{(S^{[2]}-P^{[1]})}+C^{(S^{[0]}-P^{[3]})}. \tag{15}$$

A similar issue has been seen in the discussion of the two four-derivative S-wave operators C_4 and $\widetilde{C}_4$ in the PC sector [15,55].

C. Large-N_c counting of partial-wave LECs

It is unclear how to directly count the large-N_c behavior of the partial-wave basis terms appearing in Eqs. (12) and (13); instead, the counting rules discussed in Sec. II are applied in the large-N_c basis, and Fierz transformations are used to map the scaling to the partial-wave basis operators (see the Appendix for details). The large-N_c scaling of the LECs, as well as the mapping between the LECs of the large-N_c basis and the partial-wave basis, are shown in Table I.[1] The ratios of the EFT$_{\not\pi}$ S-P LECs in the three-derivative sector that are predicted at LO in the large-N_c expansion agree with the ratios found in the one-derivative sector in Ref. [27]. In particular, the two isoscalar LECs are not independent at LO in the large-N_c expansion. Their ratio is given by

$$\frac{C_3^{(^3S_1-{}^1P_1)}}{C_{3,\Delta I=0}^{(^1S_0-{}^3P_0)}}=3\left[1+O\left(\frac{1}{N_c^2}\right)\right]. \tag{16}$$

Corrections to this identity are $O(1/N_c^2)$ because all operators suppressed by a single factor of $1/N_c$ are isovector.

[1]References [27,40] include factors of $\sin^2\theta_W$ in the counting of isovector and isotensor terms. Since these factors originate from matching at the weak scale and may be significantly modified by the nonperturbative running to the scales of EFT$_{\not\pi}$, we do not show them in this table.

For the six P-D wave transitions, the large-N_c counting rules predict that $C_3^{(^1P_1-{}^3D_1)}$, $C_{3,\Delta I=0}^{(^3P_2-{}^1D_2)}$, and $C_{3,\Delta I=2}^{(^3P_2-{}^1D_2)}$ are dominant. We see that the large-N_c behavior of the P-D LECs follows the pattern established by the S-P LECs: the $\Delta I=0$ and $\Delta I=2$ LECs are $O(N_c)$, and only one $\Delta I=0$ LEC is independent. The relationship among the $\Delta I=0$ LECs in the large-N_c expansion is predicted to be

$$\frac{C_3^{(^1P_1-{}^3D_1)}}{C_{3,\Delta I=0}^{(^3P_2-{}^1D_2)}}=3\left[1+O\left(\frac{1}{N_c^2}\right)\right]. \tag{17}$$

At LO in the large-N_c expansion, the results of Table I also predict relationships between P-D LECs and the three-derivative S-P LECs, such as

$$\frac{C_3^{(^1P_1-{}^3D_1)}}{C_3^{(^3S_1-{}^1P_1)}}=\frac{3}{4}\left[1+O\left(\frac{1}{N_c^2}\right)\right] \tag{18}$$

and

$$\frac{C_{3,\Delta I=0}^{(^3P_2-{}^1D_2)}+C_{3,\Delta I=1}^{(^3P_2-{}^1D_2)}+C_{3,\Delta I=2}^{(^3P_2-{}^1D_2)}}{C_{3,\Delta I=0}^{(^1S_0-{}^3P_0)}+C_{3,\Delta I=1}^{(^1S_0-{}^3P_0)}+C_{3,\Delta I=2}^{(^1S_0-{}^3P_0)}}=\frac{3}{4}\left[1+O\left(\frac{1}{N_c}\right)\right]. \tag{19}$$

Consistent with what is observed in Refs. [40,42,47,48], we find that the correction within a given channel is suppressed by $1/N_c^2$. The correction in Eq. (19) is $O(1/N_c)$ since the expression contains isovector LECs in addition to isoscalar and isotensor LECs.

In addition, at NLO, we obtain a large-N_c prediction for a ratio in the $\Delta I=1$ sector between the S-P and P-D channels,

$$\frac{2C_{3,\Delta I=1}^{(^3P_2-{}^1D_2)}-C_3^{(^3P_1-{}^3D_1)}+3C_3^{(^3P_2-{}^3D_2)}}{C_{3,\Delta I=1}^{(^1S_0-{}^3P_0)}+C_3^{(^3S_1-{}^3P_1)}}=\frac{3}{2}\left[1+O\left(\frac{1}{N_c^2}\right)\right]. \tag{20}$$

While we have not considered terms beyond NLO in the large-N_c expansion here, as shown in Ref. [40] all terms at NNLO in large N_c are either isoscalar or isotensor; thus corrections to the isovector identity of Eq. (20) are suppressed by $1/N_c^2$.

The impact of this section is that while there are 11 independent operators with three derivatives in EFT$_{\not\pi}$, when the accompanying LECs are ranked by powers of $1/N_c$, the 11 LECs reduce to just two that are leading in both EFT$_{\not\pi}$ and a large-N_c expansion. If nature agrees, this could provide a powerful reduction in the number of experiments needed to understand PV in NN scattering at every order in this dual expansion.

However, LECs are not observables and are generally functions of the renormalization parameter μ. Because the large-N_c predictions considered in this paper apply to LECs and not observables, care must be taken to choose a μ that both illuminates the large-N_c behavior and also obeys the power counting principles used in EFT$_{\not\pi}$. This will be discussed in the next section, along with a discussion of LEC behavior for values of μ where large-N_c relationships may not hold.

IV. RENORMALIZATION GROUP BEHAVIOR OF PV LECs

While observables must be independent of renormalization scales and schemes, the LECs of a theory in general depend upon a renormalization parameter. In the power divergence subtraction (PDS) scheme [11,12] used here, this parameter is the subtraction point μ. The dependence of the LECs on μ can be determined by requiring that observables are μ independent.

In this section, we will obtain general relationships that hold regardless of the value of μ, and will present relationships among LECs that only hold for small values of μ. The small values of μ can lead to significant simplifications for certain PV LECs, but they are likely not compatible with the LEC relationships obtained in the previous section on large N_c because of the different sizes of μ required. In what follows, we will keep the μ dependence explicit to emphasize this point.

A. Reviewing the parity-conserving renormalization group behavior

In the PC sector, the RG μ dependence of the LECs has been analyzed in detail in, for example, Refs. [11–15,55,56]. The PC Lagrangian, including the ${}^1S_0$, ${}^3S_1$, and ${}^3S_1 - {}^3D_1$ channels up to four derivatives, is (see, e.g., Ref. [15])[2]

$$\begin{aligned}\mathcal{L}^{PC} =& -C_0^{({}^3S_1)}(N^T P_i N)^\dagger (N^T P_i N) - C_0^{({}^1S_0)}(N^T P_a N)^\dagger (N^T P_a N) + \frac{1}{8}C_2^{({}^3S_1)}\big[(N^T P_i N)^\dagger (N^T P_i \overleftrightarrow{\nabla}^2 N) + \text{H.c.}\big] \\ &+ \frac{1}{8}C_2^{({}^1S_0)}\big[(N^T P_a N)^\dagger (N^T P_a \overleftrightarrow{\nabla}^2 N) + \text{H.c.}\big] + \frac{1}{4}C_2^{({}^3S_1-{}^3D_1)}\big[(N^T P_i N)^\dagger (N^T P_j \overleftrightarrow{\nabla}_x \overleftrightarrow{\nabla}_y N)\big(\delta_{ix}\delta_{jy} - \tfrac{1}{3}\delta_{ij}\delta_{xy}\big) + \text{H.c.}\big] \\ &- \frac{1}{16}C_4'^{({}^3S_1)}(N^T P_i \overleftrightarrow{\nabla}^2 N)^\dagger (N^T P_i \overleftrightarrow{\nabla}^2 N) - \frac{1}{32}\widetilde{C}_4^{({}^3S_1)}\big[(N^T P_i N)^\dagger (N^T P_i \overleftrightarrow{\nabla}^4 N) + \text{H.c.}\big] \\ &- \frac{1}{16}C_4'^{({}^1S_0)}(N^T P_a \overleftrightarrow{\nabla}^2 N)^\dagger (N^T P_a \overleftrightarrow{\nabla}^2 N) - \frac{1}{32}\widetilde{C}_4^{({}^1S_0)}\big[(N^T P_a N)^\dagger (N^T P_a \overleftrightarrow{\nabla}^4 N) + \text{H.c.}\big]. \end{aligned} \tag{21}$$

EFT$_{\not\pi}$ power counting is based on a small expansion parameter $Q/\Lambda_{\not\pi}$, where $\Lambda_{\not\pi} \sim m_\pi$ is the breakdown scale of EFT$_{\not\pi}$ and $Q \ll \Lambda_{\not\pi}$. Taking external momenta $p \sim Q$, the summation of the infinite series of loop diagrams in Fig. 1 can be justified in the PDS scheme if $|1/a - \mu| \ll \Lambda_{\not\pi}$. The LECs may be determined by matching the NN scattering amplitude to the effective range expansion about $p = 0$, yielding [11,12]

$$C_0(\mu) = \frac{4\pi}{M}\left(\frac{1}{-\mu + 1/a}\right), \tag{22}$$

$$C_2(\mu) = \frac{4\pi}{M}\left(\frac{1}{-\mu + 1/a}\right)^2 \frac{r_0}{2}, \tag{23}$$

where a is the scattering length and r_0 is the effective range for the ${}^1S_0$ or ${}^3S_1$ channels, as needed. In the following, we will continue to suppress the ${}^3S_1/{}^1S_0$ label on quantities such as C_0, C_2, a, and r_0 if they are unnecessary. The running of the S-D-mixing LEC $C_2^{({}^3S_1-{}^3D_1)}$ is governed by the RG equation [11,57]

$$\mu\frac{d}{d\mu}C_2^{({}^3S_1-{}^3D_1)}(\mu) = \frac{\mu M}{4\pi}C_0^{({}^3S_1)}(\mu)C_2^{({}^3S_1-{}^3D_1)}(\mu). \tag{24}$$

Using $E_1^{(2)} = \eta_{SD}\,(a^{({}^3S_1)})^2 + \cdots$ [58], where η_{SD} is the asymptotic SD mixing ratio, as a boundary condition for the solution to Eq. (24), $C_2^{({}^3S_1-{}^3D_1)}$ is given by [15,59]

$$C_2^{({}^3S_1-{}^3D_1)}(\mu) = -E_1^{(2)}\frac{6\sqrt{2}\pi}{M(\mu-\gamma)} = E_1^{(2)}\frac{3}{\sqrt{2}}C_0^{({}^3S_1)}(\mu). \tag{25}$$

While most applications of the EFT$_{\not\pi}$ power counting assume that $|1/a - \mu| \ll \Lambda_{\not\pi}$, Refs. [24,26,60–63] observe that the large-N_c predictions do not agree with experiment unless $\mu \gtrsim m_\pi$. At smaller values of μ, the S-wave LECs are dominated by the unnaturally large scattering lengths, which conceal the large-N_c relationships [24]. The implication is that at least in the PC sector, $\mu \gtrsim m_\pi$ may be required for this large-N_c analysis of LECs to hold. The large-N_c relationships in Sec. III C were provided without regard to the μ value. However, as we will show below, the μ dependence of the PV S-P LECs is driven by that of the PC S-wave LECs. It is therefore reasonable to expect that the PV LECs follow the pattern of PC LECs and that experimental evidence may require an imposition of $\mu \gtrsim m_\pi$ for this large-N_C analysis to hold. Fortunately, a power counting that is valid for these larger values of μ, including the justification for resumming the diagrams in Fig. 1, exists [64]; the corresponding LECs are of natural size, but the ordering of the perturbative expansion is modified compared to the case $|1/a - \mu| \ll \Lambda_{\not\pi}$.

Because the power counting for EFT$_{\not\pi}$ deviates from naive dimensional analysis in the S waves, it is important to keep distinct the mass dimension versus the power counting of operators in EFT$_{\not\pi}$. For example, both C_2 and $C_2^{({}^3S_1-{}^3D_1)}$ have mass dimension -4, but their dependence on dimensionful scales is different. From Eq. (23) and assuming that the effective range $r_0 \sim 1/\Lambda_{\not\pi}$, $C_2(\mu) \sim \frac{1}{M\widehat{\mu}^2\Lambda_{\not\pi}}$, where

$$\widehat{\mu} = \left|\mu - \frac{1}{a}\right|. \tag{26}$$

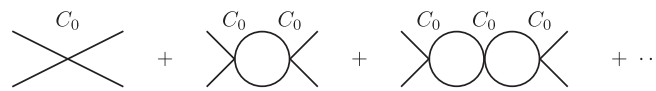

FIG. 1. Diagrams contributing to PC NN interactions at LO. C_0 can be the coupling in either the ${}^3S_1$ or ${}^1S_0$ channel.

[2]Our LEC $C_4'^{({}^3S_1)}$ is labeled ${}^{\not\pi}C_4^{({}^3S_1)}$ in Ref. [15]. Otherwise the notation is the same, except for the absence of the $\not\pi$ designation.

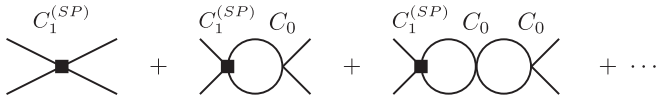

FIG. 2. The LO PV NN scattering diagrams. $C_1^{(SP)}$ is the leading weak interaction LEC and the C_0 LECs are PC. $C_1^{(SP)}$ could be any of the five LECs from Eq. (27) and C_0 is ${}^1S_0$ or ${}^3S_1$ as needed.

On the other hand, $C_2^{({}^3S_1-{}^3D_1)} \sim \frac{1}{M\widehat{\mu}\Lambda_{\not\pi}^2}$.

B. *S-P* transitions at one and three derivatives

Similar RG arguments can be applied in the PV sector. The relevant one-derivative terms in the PV Lagrangian are [27,65]

$$\begin{aligned}\mathcal{L}_{SP}^{[1]} = -\frac{1}{2}\Big[&C_1^{({}^3S_1-{}^1P_1)}(N^T P_i N)^\dagger (N^T P_0 i\overleftrightarrow{\nabla}_i N)\\ &+ C_{1,\Delta I=0}^{({}^1S_0-{}^3P_0)}(N^T P_a N)^\dagger (N^T P_{i,a} i\overleftrightarrow{\nabla}_i N)\\ &+ C_{1,\Delta I=1}^{({}^1S_0-{}^3P_0)}\epsilon_{ab3}(N^T P_a N)^\dagger (N^T P_{i,b}\overleftrightarrow{\nabla}_i N)\\ &+ C_{1,\Delta I=2}^{({}^1S_0-{}^3P_0)}\mathcal{I}_{ab}(N^T P_a N)^\dagger (N^T P_{i,b} i\overleftrightarrow{\nabla}_i N)\\ &+ C_1^{({}^3S_1-{}^3P_1)}\epsilon_{ijk}(N^T P_i N)^\dagger (N^T P_{k,3}\overleftrightarrow{\nabla}_j N)\Big] + \text{H.c.},\end{aligned} \tag{27}$$

where the subscript "1" on the LECs indicates the number of derivatives in the corresponding operator. The one-derivative Lagrangian in Eq. (27) is different from the one used in Refs. [27,65] by an overall normalization factor of 16. The reason for this is to ensure a normalization of the operators analogous to the three-derivative operators used in our large-N_c analysis. All diagrams in Fig. 2 are of the same order and must be summed to reproduce the LO PV scattering amplitude. This sum is a geometric series and simplifies to

$$\mathcal{A}_{SP}^{[1]} \propto -\,p\,C_1^{(SP)}\frac{1}{1-I_0C_0}, \tag{28}$$

where in the PDS subtraction scheme the loop integral I_0 is given by [11]

$$I_0 = -\,i\Big(\frac{\mu}{2}\Big)^{4-D}\int\frac{d^Dq}{(2\pi)^D}\frac{i}{\frac{E}{2}+q_0-\frac{\mathbf{q}^2}{2M}+i\epsilon}\frac{i}{\frac{E}{2}-q_0-\frac{\mathbf{q}^2}{2M}+i\epsilon} \overset{\text{PDS}}{=} -\frac{M}{4\pi}(\mu+ip), \tag{29}$$

with E the total energy, $p=\sqrt{ME}$ the relative momentum of the nucleons in the c.o.m. frame, and D the dimensions of spacetime used in dimensional regularization. The scattering amplitude for each channel also contains the operator structure and an overall factor, which cancels out in the RG analysis. As discussed in Ref. [65], the scattering amplitude must be independent of μ, which requires that

$$\mu\frac{d}{d\mu}\frac{C_1^{(SP)}}{C_0} = 0, \tag{30}$$

or that the ratio $C_1^{(SP)}/C_0$ is μ independent. Thus the RG running of the single-derivative PV LEC is entirely determined by that of the LO PC LEC.[3] The solution of Eq. (30) requires an undetermined integration constant that encodes the short-distance PV physics for each LEC. Assuming that only the S-wave scattering lengths are unnatural, this implies that

$$C_1^{(SP)} \sim \frac{1}{\Lambda_{\not\pi}}C_0 \sim \frac{1}{M\widehat{\mu}\Lambda_{\not\pi}}. \tag{31}$$

However, while Eq. (31) provides information on the scaling of this PV LEC with nucleon mass M, subtraction point μ, and cutoff scale $\Lambda_{\not\pi}$, there is always a dimensionless number that remains unspecified. In the present case, where we are showing the relationship between the scaling of a PV LEC and the scaling of a PC LEC, this dimensionless number involves $G_F m_\pi^2 \approx 10^{-7}$, where G_F is Fermi's coupling constant. This reflects the very different size of PV versus PC interactions, despite the fact that they scale the same with respect to μ.

The contributions to elastic PV *S-P* wave scattering from the three-derivative EFT$_{\not\pi}$ terms of Eq. (12) are shown in Fig. 3. The *S-P* scattering amplitude from three-derivative operators is

$$\mathcal{A}_{SP}^{[3]} \propto -p^3C_1^{(SP)}\frac{I_0C_2}{(1-I_0C_0)^2} - p^3C_3^{(SP)}\frac{1}{1-I_0C_0}. \tag{32}$$

Each term in Eq. (32) individually depends on μ. Requiring that the derivative of $\mathcal{A}_{SP}^{[3]}$ with respect to μ vanishes yields

$$\mu\frac{d}{d\mu}C_3^{(SP)}(\mu) = \frac{\mu M}{4\pi}\big[C_1^{(SP)}(\mu)\,C_2(\mu) + C_3^{(SP)}(\mu)\,C_0(\mu)\big]. \tag{33}$$

The solution to this equation is

$$C_3^{(SP)}(\mu) = \frac{C_1^{(SP)}(\mu)}{C_0(\mu)}C_2(\mu) + \bar{C}_3^{(SP)}\,C_0(\mu), \tag{34}$$

where $\bar{C}_3^{(SP)}$ is a new μ-independent integration constant that needs to be fixed from a lattice QCD calculation or from comparison to data. Currently, insufficient data are available to do so. (The general structure of $C_3^{(SP)}(\mu)$ in Eq. (34) was already anticipated in Ref. [65].)

While the contribution to the *S-P* scattering amplitude in Eq. (32) must be μ independent, this independence is achieved by the cancellation of the μ dependence between the two terms in Eq. (32). Substituting Eq. (34) into Eq. (32) shows that (i) the second term in Eq. (34) yields a μ-independent contribution to Eq. (32), and (ii) the first term in Eq. (34) provides the μ dependence of the second term in Eq. (32) to cancel the μ dependence in the first term of Eq. (32).

[3] At $\mu = 0, C_0(0) = 4\pi a/M$ from Eq. (22). This implies that at very low energies, the PV LEC becomes proportional to the scattering length, reminiscent of the Danilov parameters [66,67].

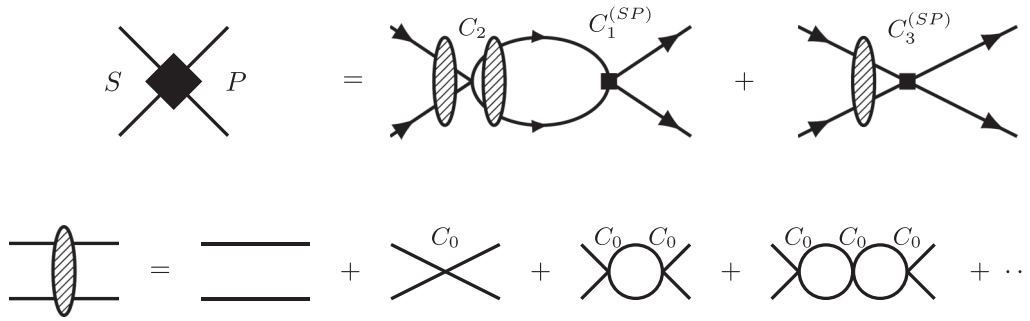

FIG. 3. The diagrams contributing to the three-derivative corrections to S-P wave transitions in EFT$_{\not\pi}$. The small squares denote insertions of PV operators with couplings $C_1^{(SP)}$ or $C_3^{(SP)}$ as indicated. The hashed ovals represent the strong S-wave rescattering, which is the sum of a noninteraction and the LO PC NN interactions.

The S-P scattering amplitude up to and including three-derivative terms is given by

$$\mathcal{A}_{SP} = \mathcal{A}_{SP}^{[1]} + \mathcal{A}_{SP}^{[3]}, \tag{35}$$

where $\mathcal{A}_{SP}^{[1]}$ and $\mathcal{A}_{SP}^{[3]}$ correspond to the contributions from the diagrams in Figs. 2 and 3, respectively, and are given by

$$\mathcal{A}_{SP}^{[1]} \propto -\frac{C_1^{(SP)}}{C_0}\frac{C_0 p}{1-I_0C_0} = -\frac{4\pi}{M}\frac{p}{\left(\frac{1}{a}+ip\right)}\underbrace{\frac{C_1^{(SP)}}{C_0}}_{\text{LO}}, \tag{36}$$

$$\begin{aligned}\mathcal{A}_{SP}^{[3]} &\propto -\frac{C_1^{(SP)}}{C_0}\frac{C_2 p^3}{(1-I_0C_0)^2} - \bar{C}_3^{(SP)}\frac{C_0 p^3}{1-I_0C_0} \\ &= -\frac{4\pi}{M}\frac{p}{\left(\frac{1}{a}+ip\right)}\left[\underbrace{\frac{C_1^{(SP)}}{C_0}\frac{r_0}{2}\frac{p^2}{\left(\frac{1}{a}+ip\right)}}_{\text{NLO}} + \underbrace{\bar{C}_3^{(SP)}p^2}_{\text{NNLO}}\right].\end{aligned} \tag{37}$$

The NLO correction to the PV scattering amplitude, which is suppressed by $Q/\Lambda_{\not\pi}$ relative to the LO contribution, is driven entirely by the leading PV LEC $C_1^{(SP)}$ and strong physics (the scattering length and the effective range parameter). No new undetermined PV parameter is required to this order; a new PV parameter is only required at NNLO.

The PC S-P scattering amplitude up to and including NLO is given by [11]

$$\mathcal{A}^{\text{PC}} = \mathcal{A}_{-1}^{\text{PC}} + \mathcal{A}_0^{\text{PC}} \propto \frac{4\pi}{M}\frac{1}{\left(\frac{1}{a}+ip\right)}\left[1+\frac{r_0}{2}\frac{p^2}{\left(\frac{1}{a}+ip\right)}\right], \tag{38}$$

where the subscripts -1 and 0 indicate the scaling with $Q/\Lambda_{\not\pi}$ in the expansion. From Eqs. (36) and (37), the PV scattering amplitude up to and including NLO is simply

$$\mathcal{A}^{\text{PV}} \propto p\frac{C_1^{(SP)}}{C_0}\mathcal{A}^{\text{PC}}. \tag{39}$$

We can apply this result to the $\vec{p}p$ longitudinal asymmetry, given by [65]

$$A_L^{\vec{p}p} = \frac{\sigma_+ - \sigma_-}{\sigma_+ + \sigma_-} = 2\frac{\text{Re}\left[\mathcal{A}^{\text{PV}}\mathcal{A}^{\text{PC}*}\right]}{|\mathcal{A}^{\text{PC}}|^2}, \tag{40}$$

where for $\vec{p}p$ scattering, $\mathcal{A}^{\text{PV}} \sim C_{1,\Delta I=0}^{(^1S_0-{}^3P_0)} + C_{1,\Delta I=1}^{(^1S_0-{}^3P_0)} + C_{1,\Delta I=2}^{(^1S_0-{}^3P_0)}$, σ is the total cross section, and the subscript $+$ or $-$ indicates the beam helicity. From Eq. (39), it is apparent that the LO asymmetry $A_L^{\vec{p}p}$ receives no NLO correction and only receives corrections at NNLO. This shows that the LO results of Ref. [65] that fit a linear combination of single-derivative LECs to the asymmetry $A_L^{\vec{p}p}$ hold through NLO.

C. S-P transitions at NNLO and beyond

The total S-P scattering amplitude is given by

$$\mathcal{A}_{SP} = \mathcal{A}_{SP}^{[1]} + \mathcal{A}_{SP}^{[3]} + \mathcal{A}_{SP}^{[5]} + \cdots. \tag{41}$$

As shown in the previous section, there is a contribution to the NNLO S-P scattering amplitude that comes from $\bar{C}_3^{(SP)}$. At the same order, there will be contributions from products of PV and PC operators containing a total of five derivatives. In particular, the scattering amplitude given by the sum of diagrams in Fig. 4 yields

$$\begin{aligned}\mathcal{A}_{SP}^{[5]} \propto -p^5\Bigg[&C_1^{(SP)}\frac{I_0C_4}{(1-I_0C_0)^2} + C_1^{(SP)}\frac{(I_0C_2)^2}{(1-I_0C_0)^3} \\ &+ C_3^{(SP)}\frac{I_0C_2}{(1-I_0C_0)^2} + C_5^{(SP)}\frac{1}{1-I_0C_0}\Bigg],\end{aligned} \tag{42}$$

where we have set $C_5^{(SP)} \equiv C^{(S^{[0]}-P^{[5]})} + C^{(S^{[2]}-P^{[3]})} + C^{(S^{[4]}-P^{[1]})}$. Following the same procedure as above, we obtain the RG equation,

$$\begin{aligned}\mu\frac{d}{d\mu}C_5^{(SP)}(\mu) = \frac{\mu M}{4\pi}\big[&C_1^{(SP)}(\mu)\,C_4(\mu) \\ &+ C_3^{(SP)}(\mu)\,C_2(\mu) + C_5^{(SP)}(\mu)\,C_0(\mu)\big].\end{aligned} \tag{43}$$

Solving this equation yields

$$C_5^{(SP)}(\mu) = \frac{C_1^{(SP)}(\mu)}{C_0(\mu)}C_4(\mu) + \bar{C}_3^{(SP)}C_2(\mu) + \bar{C}_5^{(SP)}C_0(\mu), \tag{44}$$

where $\bar{C}_5^{(SP)}$ is a new constant of integration that for naturally sized boundary conditions scales as $1/\Lambda_{\not\pi}^5$. The resulting p^5 correction to the scattering amplitude is then

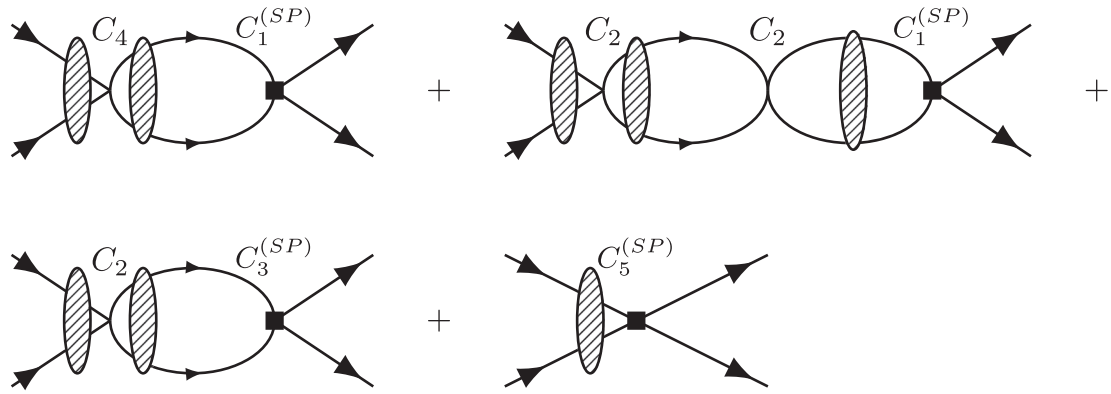

FIG. 4. The diagrams contributing to the five-derivative corrections to elastic *NN S-P* transitions in EFT$_{\not\pi}$. Notation as in Fig. 3.

given by

$$\mathcal{A}_{SP}^{[5]} \propto -p^5\left[\frac{C_1^{(SP)}}{C_0}\frac{(C_2)^2 I_0}{(1-I_0C_0)^3}+\frac{C_1^{(SP)}}{C_0}\frac{C_4}{(1-I_0C_0)^2}+\bar{C}_3^{(SP)}\frac{C_2}{(1-I_0C_0)^2}+\bar{C}_5^{(SP)}\frac{C_0}{1-I_0C_0}\right]$$
$$= -\frac{4\pi}{M}\frac{p^5}{\left(\frac{1}{a}+ip\right)}\left[\underbrace{\frac{C_1^{(SP)}}{C_0}\frac{1}{\left(\frac{1}{a}+ip\right)^2}\frac{r_0^2}{4}}_{\text{NNLO}}+\underbrace{\frac{C_1^{(SP)}}{C_0}\frac{1}{\left(\frac{1}{a}+ip\right)}\frac{r_1}{2}+\bar{C}_3^{(SP)}\frac{1}{\left(\frac{1}{a}+ip\right)}\frac{r_0}{2}}_{\text{N}^3\text{LO}}+\underbrace{\bar{C}_5^{(SP)}}_{\text{N}^4\text{LO}}\right]. \tag{45}$$

In the general case, the RG equations of these PV LECs have the form[4]

$$\mu\frac{d}{d\mu}C_{2n+1}^{(SP)} = \frac{\mu M}{4\pi}\sum_{m=0}^{n} C_{2(n-m)+1}^{(SP)} C_{2m}, \tag{46}$$

where $C_{2n+1}^{(SP)}(\mu) \equiv \sum_{m=0}^{n} C^{(S^{[2m]}-P^{[2n-2m+1]})}(\mu)$.

[4]For a given partial-wave and isospin transition, there exist several possible operator structures for a given power of momentum in the two-nucleon sector. However, all of these operator structures reduce to a single operator structure for elastic *NN* scattering. For example, the operators associated with C_4' and $\widetilde{C}_4$ both reduce to the operator for C_4. The LECs in Eq. (46) are for these single operator structures for each power of momentum in *NN* scattering.

D. *P-D* transitions

Now we consider the PV scattering amplitudes in the *P-D* channels. The four $J = 2$ *P-D* channels only receive contributions from the tree diagram [Fig. 5(a)],

$$\mathcal{A}_{^3P_2-(^{1,3})D_2}^{[3]} \propto -p^3 C_3^{(^3P_2-(^{1,3})D_2)}, \tag{47}$$

and $C_{3,\Delta I=0}^{(^3P_2-{}^1D_2)}$, $C_{3,\Delta I=1}^{(^3P_2-{}^1D_2)}$, $C_{3,\Delta I=2}^{(^3P_2-{}^1D_2)}$, and $C_3^{(^3P_2-{}^3D_2)}$ are each independent of μ. However, the $^1P_1 - {}^3D_1$ ($\Delta I = 0$) and $^3P_1 - {}^3D_1$ ($\Delta I = 1$) channels receive contributions from loop diagrams with the *S-D*-mixing parameter [Fig. 5(b)]. The corresponding scattering amplitudes are

$$\mathcal{A}_{(^{1,3})P_1-{}^3D_1}^{[3]} \propto -p^3 C_3^{((^{1,3})P_1-{}^3D_1)} - p^3 C_1^{(^3S_1-(^{1,3})P_1)}\frac{I_0 C_2^{(^3S_1-{}^3D_1)}}{1-I_0C_0}. \tag{48}$$

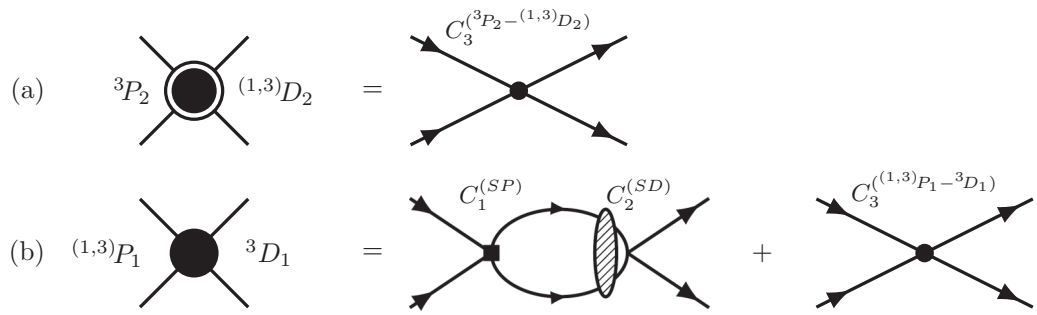

FIG. 5. The diagrams contributing to the *P-D* transitions in EFT$_{\not\pi}$. The small squares denote insertions of PV operators with couplings $C_1^{(SP)}$, and the small circles denote insertions of PV operators with couplings $C_3^{(PD)}$, as indicated. The superscript (1,3) indicates either spin singlet or spin triplet. Diagrams with strong rescattering on *P*-wave and *D*-wave channels occur at higher order.

Requiring that $\mathcal{A}^{[3]}_{(1,3)P_1-{}^3D_1}$ be μ independent and using Eq. (24), we obtain

$$\mu\frac{d}{d\mu}C_3^{((1,3)P_1-{}^3D_1)}(\mu)=\frac{\mu M}{4\pi}C_1^{({}^3S_1-(1,3)P_1)}(\mu)C_2^{({}^3S_1-{}^3D_1)}(\mu), \tag{49}$$

yielding

$$C_3^{((1,3)P_1-{}^3D_1)}(\mu)=\frac{C_1^{({}^3S_1-(1,3)P_1)}(\mu)}{C_0^{({}^3S_1)}(\mu)}C_2^{({}^3S_1-{}^3D_1)}(\mu)+\bar{C}_3^{((1,3)P_1-{}^3D_1)}, \tag{50}$$

where $\bar{C}_3^{((1,3)P_1-{}^3D_1)}$ is another μ-independent constant of integration. The structure is analogous to that of Eq. (34).

The leading contributions to the $J=1$ P-D scattering amplitudes occur at order $(Q/\Lambda_{\not\pi})^2$ in the EFT$_{\not\pi}$ power counting. Substituting Eq. (50) into Eq. (48), they are given by

$$\mathcal{A}^{[3]}_{(1,3)P_1-{}^3D_1}\propto\underbrace{-\frac{4\pi}{M}\frac{p^3}{\frac{1}{a}+ip}\frac{C_1^{({}^3S_1-(1,3)P_1)}(\mu)\,C_2^{({}^3S_1-{}^3D_1)}(\mu)}{\left[C_0^{({}^3S_1)}(\mu)\right]^2}}_{\mathrm{N^2LO}}$$

$$\underbrace{-p^3\bar{C}_3^{((1,3)P_1-{}^3D_1)}}_{\mathrm{N^3LO}}. \tag{51}$$

In addition to the contribution from $\bar{C}_3^{((1,3)P_1-{}^3D_1)}$, at the same order there are contributions to the scattering amplitudes from products of PV and PC operators containing a total of five derivatives.

E. The small μ limit

In this section, we consider the region (likely large-N_c incompatible) $|1/a-\mu|\ll\Lambda_{\not\pi}$, with $\mu\sim Q$ as well as $|1/a-\mu|\sim Q$. We will find simplifications and relationships among LECs in this limit.

1. Reviewing the small μ limit in the parity-conserving sector

At higher orders in the EFT$_{\not\pi}$ expansion, additional LECs contribute to S-wave scattering, which can be matched to higher orders in the ERE. For elastic scattering, the two LECs C_4' and $\widetilde{C}_4$ only contribute in the linear combination,

$$C_4(\mu)=C_4'(\mu)+\widetilde{C}_4(\mu)$$
$$=\frac{4\pi}{M}\frac{r_0^2}{4}\left(\frac{1}{-\mu+1/a}\right)^3+\frac{4\pi}{M}\frac{r_1}{2\Lambda_{\not\pi}^2}\left(\frac{1}{-\mu+1/a}\right)^2, \tag{52}$$

where $r_1/\Lambda_{\not\pi}^2$ is the shape parameter in the relevant (spin-singlet or spin-triplet) channel [11]. We are again suppressing ${}^1S_0$ and ${}^3S_1$ labels as Eq. (52) is valid for both. If both r_0 and r_1 are of natural size, that is, if they both scale as $1/\Lambda_{\not\pi}$, the first term in Eq. (52) scales as $\frac{1}{M\widehat{\mu}^3\Lambda_{\not\pi}^2}$ and the second as $\frac{1}{M\widehat{\mu}^2\Lambda_{\not\pi}^3}$, where again $\widehat{\mu}=|\mu-1/a|$. So long as $|1/a-\mu|\ll\Lambda_{\not\pi}$, the second term is suppressed relative to the first by a factor of $\widehat{\mu}/\Lambda_{\not\pi}$. If this term is neglected, the LEC C_4 is entirely determined from the scattering length and the effective range and no new parameter enters. In general, if $|1/a-\mu|\ll\Lambda_{\not\pi}$ and all parameters aside from the scattering length are of natural size (that is, they scale with inverse mass dimension $\Lambda_{\not\pi}$), the "leading" (in a $\widehat{\mu}/\Lambda_{\not\pi}$ expansion) behavior for C_{2n} is

$$C_{2n}(\mu)\sim\frac{1}{M\widehat{\mu}^{n+1}\Lambda_{\not\pi}^n}, \tag{53}$$

where $n>0$ and $2n$ is the number of derivatives associated with the operator for the C_{2n} LEC [11,18].

2. The small μ limit for S-P transitions at three derivatives

If there are no other as-yet-unidentified unnatural scales in the problem, $\bar{C}_3^{(SP)}$ in Eq. (34) should scale as $1/\Lambda_{\not\pi}^3$, again keeping in mind that this is the scaling with dimensionful parameters in the theory; the very different sizes of PV versus PC LECs are encoded in a dimensionless proportionality constant involving $G_F m_\pi^2$, as discussed in Sec. IV B. The first term in Eq. (34) scales as $\frac{1}{M\widehat{\mu}^2\Lambda_{\not\pi}^2}$, while the second term scales as $\frac{1}{M\widehat{\mu}\Lambda_{\not\pi}^3}$.

As long as $\widehat{\mu}=|\mu-1/a|\ll\Lambda_{\not\pi}$, it is useful to expand Eq. (34) as

$$C_3^{(SP)}(\mu)=\frac{C_1^{(SP)}(\mu)}{C_0(\mu)}C_2(\mu)\left[1+O\left(\frac{\widehat{\mu}}{\Lambda_{\not\pi}}\right)\right]. \tag{54}$$

In this case, the term with $\bar{C}_3^{(SP)}$ is suppressed by a factor of $\widehat{\mu}/\Lambda_{\not\pi}$ and can be neglected; $C_3^{(SP)}$ is dominated by the LO PV LEC $C_1^{(SP)}$ and the PC LECs C_0 and C_2. For $\widehat{\mu}\gtrsim\Lambda_{\not\pi}$, which is the domain in which the large-N_c relationships are expected to hold, both terms in Eq. (34) are expected to be of the same size, and the expansion of Eq. (54) breaks down; $\bar{C}_3^{(SP)}$ cannot be neglected.

3. The small μ limit of S-P transitions at NNLO and beyond

The complete solution to Eq. (46) requires integration constants that must be fit to experiment or lattice calculations, which are currently unavailable. However, assuming that the integration constant $\bar{C}_{2n+1}^{(SP)}\sim 1/\Lambda_{\not\pi}^{2n+1}$, the leading behavior of PV LECs for $|1/a-\mu|\ll\Lambda_{\not\pi}$ is

$$C_{2n+1}^{(SP)}(\mu)\equiv\sum_{m=0}^{n}C^{({}^{S^{[2m]}}-{}^{P^{[2n-2m+1]}})}(\mu)$$
$$=\frac{C_1^{(SP)}(\mu)}{C_0(\mu)}C_{2n}(\mu)\left[1+O\left(\frac{\widehat{\mu}}{\Lambda_{\not\pi}}\right)\right]. \tag{55}$$

By analogy with the discussion of PC LECs in Ref. [11], Eq. (55) implies that the leading behavior of PV LECs for $n>0$ is driven only by the PV observable $C_1^{(SP)}/C_0$ and the S-wave strong interaction LECs in the small μ limit. But this does not mean that PV observables can be determined beyond NLO with $C_1^{(SP)}$ alone; at NNLO and beyond, higher-order PV parameters must be included.

4. LEC relationships in the small μ limit

Again, if the constant term in Eq. (50) is assumed to be of natural size and if $|1/a^{({}^3S_1)}-\mu|\ll\Lambda_{\not\pi}$, $\bar{C}_3^{((1,3)P_1-{}^3D_1)}$ is suppressed by $\widehat{\mu}/\Lambda_{\not\pi}$, where $\widehat{\mu}=|\mu-1/a|$, compared to the

other term in Eq. (50). For this restriction on μ, we can write

$$\frac{C_3^{(^1P_1-^3D_1)}(\mu)}{C_2^{(^3S_1-^3D_1)}(\mu)} = \frac{C_1^{(^3S_1-^1P_1)}(\mu)}{C_0^{(^3S_1)}(\mu)}\left[1+O\left(\frac{\widehat{\mu}}{\Lambda_{\not\pi}}\right)\right]. \quad (56)$$

This implies that the leading contribution of $C_3^{(^1P_1-^3D_1)}$ is determined by PC LECs and a LO PV LEC. A constraint on $C_1^{(^3S_1-^1P_1)}$ can be extracted from the recent NPDGamma measurement [32], using the result from Ref. [68]. After adjusting for the different normalization of the operators, we find, for $|1/a^{(^3S_1)}-\mu| \ll \Lambda_{\not\pi}$,

$$\frac{C_3^{(^3P_1-^3D_1)}}{C_2^{(^3S_1-^3D_1)}}+O\left(\frac{\widehat{\mu}}{\Lambda_{\not\pi}}\right) \approx \frac{C_1^{(^3S_1-^3P_1)}}{C_0^{(^3S_1)}} = (-7.3\pm 3.4\pm 0.5)\times 10^{-10}\ \mathrm{MeV}^{-1}. \quad (57)$$

In the above equation, we list just the experimental (statistical plus systematic) errors from the NPDGamma experiment [32]. For the equality, the associated EFT$_{\not\pi}$ errors are $Q/\Lambda_{\not\pi}$. Corrections to the approximation are roughly 30% for $\widehat{\mu}\sim Q$ and include a contribution from $\bar{C}_3^{(^3P_1-^3D_1)}$ (they could be 100% if $\widehat{\mu}$ is large).

5. *Expansion around the deuteron pole*

For processes involving the $^3S_1$ channel, it is useful to consider the effective range expansion about the deuteron pole [69,70]. For this case, the PC LECs are expanded in powers of Q. For example, $C_0 = C_{0,-1}+C_{0,0}+C_{0,1}+\cdots$, where, on the right-hand side, the first and second subscripts indicate the number of derivatives of the operator, and the order in powers of Q, respectively. The μ-scaling of these PC LECs, including relativistic corrections, is given in Ref. [15]. Similarly, we can express the PV LECs as a power series in Q, e.g., $C_1^{(SP)} = C_{1,-1}^{(SP)}+C_{1,0}^{(SP)}+C_{1,1}^{(SP)}+\cdots$. We verified that the RG behaviors of the PV LECs in the deuteron pole expansion can be analyzed order by order by following the same procedures we used above, and the arguments about which LECs are dominant in the range $|1/a-\mu| \ll \Lambda_{\not\pi}$ are similar.

V. CONCLUSIONS

We analyzed the three-derivative parity-violating NN contact interactions in the dual EFT$_{\not\pi}$ and large-N_c expansion. The minimal set of three-derivative EFT$_{\not\pi}$ operators for elastic scattering consists of five that correct the (five) LO S-P transitions and six that describe the leading contribution to the P-D transitions. The LECs accompanying these operators are free parameters in EFT$_{\not\pi}$ and must be fit to the experimental data or extracted from lattice QCD. The large-N_c expansion reduces the number of independent LECs at a given order, either by demoting some to higher order in the dual EFT$_{\not\pi}$ and large-N_c expansion or by relating some LECs to each other. By organizing the LECs of the three-derivative operators in EFT$_{\not\pi}$ in powers of $1/N_c$, we can establish a hierarchy among them. The isoscalar and isotensor LECs appear at LO in N_c, while four isovector LECs appear at subleading order in N_c. The relationships found among the LECs hold up to corrections of $1/N_c^2\sim 10\%$ channel by channel. The relationships among the LECs for three-derivative S-P operators echo those found in the one-derivative sector; in both cases, the two isoscalar LECs are not independent, and isoscalar and isotensor terms dominate in the large-N_c limit. For elastic scattering, the 11 independent LECs that occur at three derivatives in EFT$_{\not\pi}$ are reduced to two at LO in the dual EFT$_{\not\pi}$ and large-N_c expansion. This may provide constraints that can be checked by future experiments and lattice QCD calculations. As usual, because $N_c=3$ in our world, a large-N_c treatment cannot offer exact predictions, but should indicate general trends.

We also studied the RG behavior of the three-derivative operators and analyzed the running of the PV LECs with respect to the subtraction point μ. For μ in the range $|1/a-\mu| \ll \Lambda_{\not\pi}$, the leading behavior of all the S-P LECs only depends on $C_1^{(SP)}$ and the strong S-wave LECs. The analysis of the P-D LECs shows that $^3S_1-{}^3D_1$ mixing introduces μ dependence in the $J=1$ P-D LECs, while the $J=2$ P-D LECs are μ independent. This RG analysis allows us to power count PV NN scattering operators in EFT$_{\not\pi}$; it indicates that some previous (LO) calculations of S-P channel observables [65] do not obtain corrections until NNLO. It also shows that LECs in two $J=1$ P-D channels are related to S-P LECs for sufficiently small values of μ. We emphasize again that the value of μ needed for large-N_c relationships to hold may be incompatible with the small values of $|1/a-\mu|$ that lead to some simplifications of the RG relationships. While we address two distinct regions of μ in this paper, we anticipate that one or the other may be useful for reducing the number of independent LECs required to analyze a given process.

ACKNOWLEDGMENTS

The request to find large-N_c constraints on P-D wave operators was made by the participants of the KITP Workshop on Hadronic Parity Nonconservation (Santa Barbara, CA (2018)). S.T.N. thanks H. Singh for many insightful suggestions and guidance throughout this project. R.P.S. thanks H. Singh for useful discussions and for his mentorship of S.T.N. This material is based upon work supported by the U.S. Department of Energy, Office of Science, Office of Nuclear Physics, under Award No. DE-FG02-05ER41368 (S.T.N. and R.P.S.), and Award No. DE-SC0019647 (M.R.S.).

APPENDIX: FIERZ TRANSFORMATION

In this section, we show in detail one method for matching between the large-N_c and partial-wave bases using Fierz identities. The relevant Fierz identities are

$$\delta_{AB}\delta_{CD} = \tfrac{1}{2}(\sigma_2)_{CA}(\sigma_2)_{BD}+\tfrac{1}{2}(\sigma_i\sigma_2)_{CA}(\sigma_2\sigma_i)_{BD},$$
$$(\sigma_i)_{AB}\delta_{CD} = -\tfrac{1}{2}[(\sigma_i\sigma_2)_{CA}(\sigma_2)_{BD}+(\sigma_2)_{CA}(\sigma_2\sigma_i)_{BD}]$$

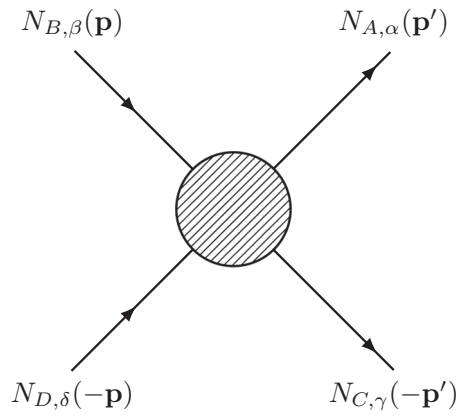

FIG. 6. Assignment of spin, isospin indices and momenta. Greek letters denote isospin indices and uppercase Latin letters denote spin indices.

$$
\begin{aligned}
&- \tfrac{1}{2} i\epsilon_{ijk}(\sigma_j\sigma_2)_{CA}(\sigma_2\sigma_k)_{BD},\\
(\sigma_i)_{AB}(\sigma_j)_{CD} = &- \tfrac{1}{2}\delta_{ij}(\sigma_2)_{CA}(\sigma_2)_{BD} + \tfrac{1}{2} i\epsilon_{ijk}\big[(\sigma_k\sigma_2)_{CA}(\sigma_2)_{BD}\\
&- (\sigma_2)_{CA}(\sigma_2\sigma_k)_{BD}\big]\\
&- \tfrac{1}{2}(\delta_{ik}\delta_{jn} + \delta_{in}\delta_{jk} - \delta_{ij}\delta_{kn})(\sigma_k\sigma_2)_{CA}(\sigma_2\sigma_n)_{BD},
\end{aligned}
\tag{A1}
$$

where the uppercase Latin letters denote spin indices. These formulas are also applied to isospin matrices by substituting $\sigma \to \tau$. One approach to performing Fierz transformations is to take matrix elements, as outlined in Appendix A of Ref. [65]. For example, the matrix element of the operator corresponding to $\widetilde{C}^{[3]}_{G.G}$ in Eq. (10) (see Fig. 6 for momentum and index assignments) is

$$
\begin{aligned}
\langle \widetilde{\mathcal{O}}^{[3]}_{G.G} \rangle = &\, 2\epsilon_{ijk}[(\sigma_i)_{AB}(\sigma_l)_{CD} + (\sigma_l)_{AB}(\sigma_i)_{CD}]\epsilon_{ab3}(\tau_a)_{\alpha\beta}(\tau_b)_{\gamma\delta}(p_i + p_i')(p_k - p_k')(p_l - p_l')\\
&- 2\epsilon_{ijk}[(\sigma_i)_{CB}(\sigma_l)_{AD} + (\sigma_l)_{CB}(\sigma_i)_{AD}]\epsilon_{ab3}(\tau_a)_{\gamma\beta}(\tau_b)_{\alpha\delta}(p_i - p_i')(p_k + p_k')(p_l + p_l').
\end{aligned}
\tag{A2}
$$

The operator symbol in the matrix element above echoes its corresponding LEC; e.g., $\widetilde{\mathcal{O}}^{[3]}_{G.G}$ is the operator associated with $\widetilde{C}^{[3]}_{G.G}$. Applying the identities in Eq. (A1) gives

$$
\langle \widetilde{\mathcal{O}}^{[3]}_{G.G} \rangle = 64 i\epsilon_{ijk}(\delta_{im}\delta_{ln} + \delta_{in}\delta_{lm})(P_m^\dagger)_{CA,\gamma\alpha}(P_{n,3})_{BD,\beta\delta}(p_j p_k' p_l') + \text{H.c.}
\tag{A3}
$$

This structure suggests that the $\widetilde{C}^{[3]}_{G.G}$ term may contribute to ${}^3S_1 - {}^3P_1$, ${}^3P_1 - {}^3D_1$, and ${}^3P_2 - {}^3D_2$ transitions. The corresponding partial-wave matrix elements for these three channels are

$$
\langle \mathcal{O}^{[3]}_{{}^3S_1 - {}^3P_1} \rangle = -4C_3^{({}^3S_1 - {}^3P_1)}\, i\epsilon_{ijk}(P_i^\dagger)_{CA,\gamma\alpha}(P_{j,3})_{BD,\beta\delta}(p'^2 p_k) + \text{H.c.},
\tag{A4}
$$

$$
\begin{aligned}
\langle \mathcal{O}^{[3]}_{{}^3P_1 - {}^3D_1} \rangle = &-4C_3^{({}^3P_1 - {}^3D_1)}\, i\epsilon_{ijk}(P_l^\dagger)_{CA,\gamma\alpha}(P_{i,3})_{BD,\beta\delta}(p_l' p_k' p_j)\\
&+ \frac{4}{3} C_3^{({}^3P_1 - {}^3D_1)}\, i\epsilon_{ijk}(P_i^\dagger)_{CA,\gamma\alpha}(P_{j,3})_{BD,\beta\delta}(p'^2 p_k) + \text{H.c.},
\end{aligned}
\tag{A5}
$$

$$
\begin{aligned}
\langle \mathcal{O}^{[3]}_{{}^3P_2 - {}^3D_2} \rangle = &-4C_3^{({}^3P_2 - {}^3D_2)}\, i\epsilon_{ijk}(P_i^\dagger)_{CA,\gamma\alpha}(P_{j,3})_{BD,\beta\delta}(p_k' p_l' p_l)\\
&- 4C_3^{({}^3P_2 - {}^3D_2)}\, i\epsilon_{ijk}(P_i^\dagger)_{CA,\gamma\alpha}(P_{l,3})_{BD,\beta\delta}(p_k' p_l' p_j) + \text{H.c.},
\end{aligned}
\tag{A6}
$$

where the projectors P_x are defined in Eq. (14). Using

$$
\begin{aligned}
\epsilon_{ijk}(P_i^\dagger)_{CA,\gamma\alpha}(P_{j,3})_{BD,\beta\delta}(p_k' p_l' p_l) = &\, \epsilon_{ijk}(P_i^\dagger)_{CA,\gamma\alpha}(P_{j,3})_{BD,\beta\delta}(p_k p'^2) + \epsilon_{ijk}(P_i^\dagger)_{CA,\gamma\alpha}(P_{l,3})_{BD,\beta\delta}(p_k' p_l' p_j)\\
&- \epsilon_{ijk}(P_l^\dagger)_{CA,\gamma\alpha}(P_{i,3})_{BD,\beta\delta}(p_k' p_l' p_l)
\end{aligned}
\tag{A7}
$$

with Eq. (A3) yields

$$
\langle \widetilde{\mathcal{O}}^{[3]}_{G.G} \rangle = -24\langle \mathcal{O}^{[3]}_{{}^3P_1 - {}^3D_1} \rangle - 8\langle \mathcal{O}^{[3]}_{{}^3P_2 - {}^3D_2} \rangle.
\tag{A8}
$$

[1] S.-L. Zhu, C. M. Maekawa, B. R. Holstein, M. J. Ramsey-Musolf, and U. van Kolck, Nucl. Phys. A **748**, 435 (2005).

[2] M. J. Ramsey-Musolf and S. A. Page, Ann. Rev. Nucl. Part. Sci. **56**, 1 (2006).

[3] W. C. Haxton and B. R. Holstein, Prog. Part. Nucl. Phys. **71**, 185 (2013).

[4] M. R. Schindler and R. P. Springer, Prog. Part. Nucl. Phys. **72**, 1 (2013).

[5] S. Gardner, W. C. Haxton, and B. R. Holstein, Ann. Rev. Nucl. Part. Sci. **67**, 69 (2017).

[6] J. Wasem, Phys. Rev. C **85**, 022501 (2012).

[7] T. Kurth, E. Berkowitz, E. Rinaldi, P. Vranas, A. Nicholson, M. Strother, A. Walker-Loud, and E. Rinaldi, PoS (Lattice 2015) **251**, 329 (2016).

[8] D. B. Kaplan, M. J. Savage, and M. B. Wise, Nucl. Phys. B **478**, 629 (1996).

[9] P. F. Bedaque and U. van Kolck, Phys. Lett. B **428**, 221 (1998).
[10] U. van Kolck, Lect. Notes Phys. **513**, 62 (1998).
[11] D. B. Kaplan, M. J. Savage, and M. B. Wise, Nucl. Phys. B **534**, 329 (1998).
[12] D. B. Kaplan, M. J. Savage, and M. B. Wise, Phys. Lett. B **424**, 390 (1998).
[13] M. C. Birse, J. A. McGovern, and K. G. Richardson, Phys. Lett. B **464**, 169 (1999).
[14] U. van Kolck, Nucl. Phys. A **645**, 273 (1999).
[15] J.-W. Chen, G. Rupak, and M. J. Savage, Nucl. Phys. A **653**, 386 (1999).
[16] U. van Kolck, Prog. Part. Nucl. Phys. **43**, 337 (1999).
[17] S. R. Beane, P. F. Bedaque, W. C. Haxton, D. R. Phillips, and M. J. Savage, in *At The Frontier of Particle Physics: Handbook Of QCD*, edited by M. Shifman, Vol. 1 (World Scientific, Singapore, 2001), pp. 133–269.
[18] P. F. Bedaque and U. van Kolck, Ann. Rev. Nucl. Part. Sci. **52**, 339 (2002).
[19] L. Platter, Few Body Syst. **46**, 139 (2009).
[20] U. van Kolck, in *Proc. 2017 Les Houches Summer School: EFT in Particle Physics and Cosmology, Les Houches, France, 2019*, edited by S. Davidson, P. Gambino, M. Laine, M. Neubert, and C. Salomon, Vol. 108 (Oxford University Press, Oxford, 2020).
[21] H.-W. Hammer, S. König, and U. van Kolck, Rev. Mod. Phys. **92**, 025004 (2020).
[22] G. Hooft, Nucl. Phys. B **72**, 461 (1974).
[23] E. Witten, Nucl. Phys. B **160**, 57 (1979).
[24] D. B. Kaplan and M. J. Savage, Phys. Lett. B **365**, 244 (1996).
[25] D. B. Kaplan and A. V. Manohar, Phys. Rev. C **56**, 76 (1997).
[26] M. R. Schindler, H. Singh, and R. P. Springer, Phys. Rev. C **98**, 044001 (2018).
[27] M. R. Schindler, R. P. Springer, and J. Vanasse, Phys. Rev. C **93**, 025502 (2016) [Erratum: **97**, 059901 (2018)].
[28] J. Vanasse and A. David, arXiv:1910.03133.
[29] T. R. Richardson and M. R. Schindler, Phys. Rev. C **101**, 055505 (2020).
[30] P. D. Eversheim *et al.*, Phys. Lett. B **256**, 11 (1991).
[31] W. Haeberli and B. R. Holstein, in *Symmetries And Fundamental Interactions In Nuclei*, edited by W. Haxton and E. Henley (World Scientific, Singapore, 1995), pp. 17–66.
[32] D. Blyth *et al.* (NPDGamma), Phys. Rev. Lett. **121**, 242002 (2018).
[33] A. R. Berdoz *et al.* (TRIUMF E497), Phys. Rev. Lett. **87**, 272301 (2001).
[34] A. R. Berdoz *et al.* (TRIUMF E497), Phys. Rev. C **68**, 034004 (2003).
[35] V. A. Knyaz'kov, E. A. Kolomensky, V. M. Lobashev, V. A. Nazarenko, A. N. Pirozhkov, Yu. V. Sobolev, A. I. Shablii, and E. V. Shulgina, JETP Lett. **38**, 163 (1983).
[36] V. A. Knyaz'kov, E. Kolomenskii, V. Lobashov, V. Nazarenko, A. Pirozhkov *et al.*, Nucl. Phys. A **417**, 209 (1984).
[37] M. W. Ahmed, A. E. Champagne, B. R. Holstein, C. R. Howell, W. M. Snow, R. P. Springer, and W. K. Wu, in *Community Summer Study 2013: Snowmass on the Mississippi* (2013), arXiv:1307.8178.
[38] C. R. Howell *et al.*, arXiv:2012.10843.
[39] S. R. Beane and M. J. Savage, Nucl. Phys. B **636**, 291 (2002).
[40] D. R. Phillips, D. Samart, and C. Schat, Phys. Rev. Lett. **114**, 062301 (2015).
[41] E. E. Jenkins, Ann. Rev. Nucl. Part. Sci. **48**, 81 (1998).
[42] A. V. Manohar, in *Les Houches Summer School in Theoretical Physics, Session 68: Probing the Standard Model of Particle Interactions* (1998), pp. 1091–1169, arXiv:hep-ph/9802419.
[43] R. F. Lebed, Mesons and light nuclei. Proceedings of the 11th Indian-Summer School on Intermediate-Energy Physics, Prague, Czech Republic, September 7-11, 1998, Czech. J. Phys. **49**, 1273 (1999).
[44] J.-L. Gervais and B. Sakita, Phys. Rev. Lett. **52**, 87 (1984).
[45] R. F. Dashen and A. V. Manohar, Phys. Lett. B **315**, 425 (1993).
[46] R. F. Dashen and A. V. Manohar, Phys. Lett. B **315**, 438 (1993).
[47] R. F. Dashen, E. E. Jenkins, and A. V. Manohar, Phys. Rev. D **51**, 3697 (1995).
[48] R. Dashen, E. Jenkins, and A. V. Manohar, Phys. Rev. D **49**, 4713 (1994), [Erratum: **51**, 2489 (1995)].
[49] E. E. Jenkins, Phys. Lett. B **315**, 431 (1993).
[50] E. E. Jenkins, Phys. Lett. B **315**, 441 (1993).
[51] M. K. Banerjee, T. D. Cohen, and B. A. Gelman, Phys. Rev. C **65**, 034011 (2002).
[52] D. Samart, C. Schat, M. R. Schindler, and D. R. Phillips, Phys. Rev. C **94**, 024001 (2016).
[53] M. Tanabashi *et al.* (Particle Data Group), Phys. Rev. D **98**, 030001 (2018).
[54] S. Fleming, T. Mehen, and I. W. Stewart, Nucl. Phys. A **677**, 313 (2000).
[55] G. Rupak, Nucl. Phys. A **678**, 405 (2000).
[56] T. Mehen and I. W. Stewart, Phys. Lett. B **445**, 378 (1999).
[57] S. Fleming, T. Mehen, and I. W. Stewart, Phys. Rev. C **61**, 044005 (2000).
[58] J.-W. Chen, G. Rupak, and M. J. Savage, Phys. Lett. B **464**, 1 (1999).
[59] J. Vanasse, Phys. Rev. C **88**, 044001 (2013).
[60] T. Mehen, I. W. Stewart, and M. B. Wise, Phys. Rev. Lett. **83**, 931 (1999).
[61] A. Calle Cordon and E. Ruiz Arriola, Phys. Rev. C **78**, 054002 (2008).
[62] A. Calle Cordon and E. Ruiz Arriola, Phys. Rev. C **80**, 014002 (2009).
[63] E. Ruiz Arriola, Symmetry **8**, 42 (2016).
[64] E. Epelbaum, J. Gegelia, and U.-G. Meißner, Nucl. Phys. B **925**, 161 (2017).
[65] D. R. Phillips, M. R. Schindler, and R. P. Springer, Nucl. Phys. A **822**, 1 (2009).
[66] G. Danilov, Phys. Lett. **18**, 40 (1965).
[67] G. Danilov, Phys. Lett. B **35**, 579 (1971).
[68] M. R. Schindler and R. P. Springer, Nucl. Phys. A **846**, 51 (2010).
[69] H. A. Bethe, Phys. Rev. **76**, 38 (1949).
[70] H. A. Bethe and C. Longmire, Phys. Rev. **77**, 647 (1950).